Mining of Mineral Deposits
Volume 17 (2023), Issue 1, 43-50

https://doi.org/10.33271/mining17.01.043

Improving a technique to calculate strength of cylindrical rock samples in terms of uniaxial compression

Leonid Vasyliev[1], Mykola Malich[2*], Dmytro Vasyliev[1], Volodymyr Katan[3], Zahar Rizo[1]

[1] *Institute of Geotechnical Mechanics named by N. Poljakov of National Academy of Sciences of Ukraine, Dnipro, Ukraine*
[2] *Ukrainian State University of Science and Technology, Dnipro, Ukraine*
[3] *Oles Honchar Dnipro National University, Dnipro, Ukraine*

**Corresponding author: e-mail n22051957m@gmail.com*

Abstract

Purpose is to improve analytical technique to calculate strength of cylindrical rock samples taking into consideration standard horizontal stresses.

Methods. Mathematical modeling of cylindrical rock sample breakage under the truncated-wedge destruction was performed taking into consideration the standard horizontal stresses using four experimental characteristics (i.e. k being shear strength; f_c and μ being contact and internal friction coefficients; and E being elasticity modulus) as well as comparing the design strength with experimental data obtained in the process of uniaxial compression.

Findings. The technique makes it possible to identify both maximum strength and residual strength of cylindrical rock samples using four indicators of properties which can be simply defined by experiment. Comparison of the analytical strength limits and experimental data, obtained in terms of uniaxial compression, supports the idea of high efficiency of the proposed technique.

Originality. For the first time, analytical modeling of cylindrical rock sample breakage has been performed in terms of the truncated-wedge destruction taking into consideration the standard horizontal stresses as well as contact and internal friction parameters.

Practical implications. The technique advantage is to apply promptly the calculation results in the context of industrial enterprises since their environment helps apply simple procedures to define indices of physicomechanical characteristics of rocks for determination of stability of underground structures and reduction of energy consumption while disintegrating in open pits and mining and processing complexes.

Keywords: *rock, strength, breakage, crack, stress, uniaxial compression*

1. Introduction

Physicomechanical characteristics of both mined and associated rocks are among the most important information data required to control stress and strained state of rock mass and identify stability of underground structures especially concerning face areas [1], [2]. The rock characteristics are also used while mineral processing; it especially concerns ore material preparation from the viewpoint of mining and smelting procedures, preparation of building materials, chemical production etc. In this context, the improved efficiency of rock mass and another hard material destruction with a reduction in energy costs is the most topical issue [3]. First of all, it concerns mines, open pits, mining and processing integration works, stone-processing enterprises, processing of structural components of the complexes on emergency procedures etc. In the process of the problem solving, strength of prismatic and cylindrical samples of the studied materials as well as their residual strength, determined in terms of axial stress-strain diagrams of their evanescent destruction, is the most important material capability [4]-[6]. The information is essential for core cylindrical samples obtained at mining enterprises while drilling since the data may be used promptly in operation.

Despite the advantage of such experimental diagrams, developed by different authors using various rocks from various open pits and mines, they cannot ensure sufficient reliability of bearing capacity of rock masses [7]-[9] since the diagrams, distinguishing in their types for different rocks and sample dimensions, are only external characteristics. They prevent from revealing of internal local processes of progressive cracks starting the process when certain share of the material is getting beyond the load varying the bearing capacity of the sample as well as rock mass; from describing geometry of the cracks and regularities of changes in vertical stresses within their points. Hence, to understand internal processes of evanescent curve formation, it is desirable to "look within" a sample, and evaluate the phenomena taking place there [7].

Received: 7 May 2021. Accepted:27 January 2023. Available online: 30 March 2023

Mining of Mineral Deposits. ISSN 2415-3443 (Online) | ISSN 2415-3435 (Print)

Researchers mention that rock masses are characterized by high values of horizontal stresses [10], [11] playing a key role while assessing stress and strain state (SSS) of the rock masses [12], [13]. However, it is not clear how to assess the impact. Hence, it is required to develop an analytical technique helping calculate both limits and residual strength of samples with the knowledge of indicators of rock properties defined with the help of simple procedures being accessible for mining enterprises. Earlier, attempts have been made to simulate mathematically the processes of sample breakage [1], [8], [13]. In such a way, paper [13] bases theoretical substantiation of bearing capability of extraction pillars and mine workings on the approximation of evanescent curves relying upon different hypotheses and methods of plasticity theory, i.e. the associated flow law of the limit state under plain and axisymmetric deformation. Immediately, the design schemes are complemented by the values of horizontal stresses σ_x assuming antecedently their availability within the rock mass. In this regard, uniform distribution of rock pressure, being equal to γH, is adopted on the contact plains. A deformation curve is described by means of a piecewise approximation while emphasizing that experimental data approximation may involve piecewise-linear dependencies having horizontal asymptotes. Earlier, certain efforts have also been made to simulate mathematically rock breakage processes [14]-[17]. Nevertheless, the models have not been perfected to the level of the completed analytical methods calculating strength of rock samples.

Prismatic or cylindrical samples are applied to identify rock strength experimentally. Book [18] elaborates methods of analytical strength determination for prismatic samples. Maybe, cylindrical core drilling samples are more popular than prismatic samples while determining experimental strength limits. Hence, the necessity arises to develop analytical techniques calculating strength for cylindrical samples. Paper [19] has developed analytical procedure to calculate parameters of stress-strain diagrams in terms of cylindrical samples where the truncated-wedge destruction was applied. However, the technique has several disadvantages. One of them is impossibility to take into consideration the standard horizontal stresses resulting inevitably from the contact pressure between a press plate and sample while developing their fracture diagrams. Secondly, paper [19] has proposed following distribution formula for the standard contact stresses as applied to a cylinder circle (Fig. 1):

$$\sigma_{yi} = \sigma_{y0}\left(\frac{2\sqrt{ux - x^2}}{u} + \frac{4 f_c}{uh} x\sqrt{ux - x^2}\right), \qquad (1)$$

where:

σ_{yi} – current standard vertical stress on the contact sample plain, Pa;

σ_{y0} – standard vertical stress within the angular point of a sample, Pa;

f_c – contact friction coefficient;

x – abscissa within the considered point;

h – sample height;

u – diameter of a cylinder circle.

Prandtl formula on the contact stress distribution for prismatic unitary width sample has been applied as an analogue [18]:

$$\sigma_{yi} = \sigma_{y_0}\left(1 + \frac{2 f_c \cdot x}{h}\right). \qquad (2)$$

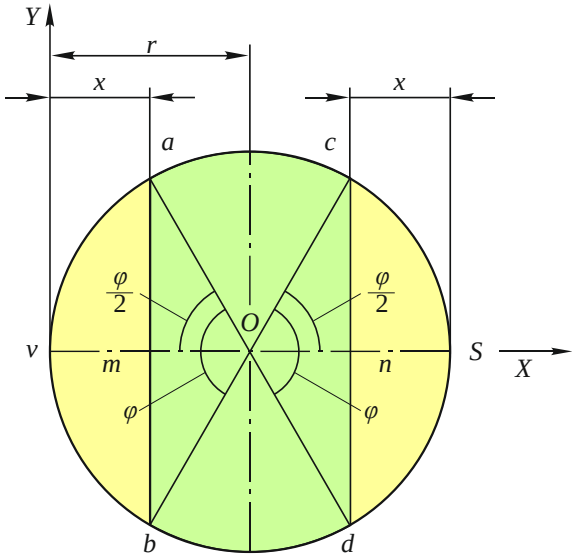

Figure 1. Scheme of the bearing surface shaping during symmetrical crack development within a cylindrical sample

Nevertheless, record (1) of stress distribution has a disadvantage. Under boundary conditions $x = 0$, stress is $\sigma_{yi} = 0$ instead of $\sigma_{yi} = \sigma_{y0}$ as it occurs in terms of Formula (2). Consequently, the contact stress distribution record for a circle should be revised. The improvement of contact stress distribution needs derivation of new analytical mathematical expressions to define specific efforts on the contact surfaces between the plates and a sample to compare with calculation results of the efforts stated by paper [19]. Moreover, it is important to involve the impact of horizontal stresses, resulting from shear stresses and being shaped by the contact friction, on the sample strength.

Relying upon the abovementioned, the paper formulates following tasks:

1) improve the analytical technique to identify parameters of axial stress-strain diagrams under the truncated-wedge destruction of cylindrical rock samples using their four experimental characteristics which can be defined in laboratories of mining enterprises;

2) involve in the calculation procedure the impact of horizontal stresses on the sample stress and substantiate it relying upon the specified distribution of the standard contact stresses;

3) compare convergences of the design data with the experimental data ignoring the standard horizontal stresses, resulting from shear stresses and being shaped by the contact friction, and taking them into consideration.

2. The research methods

Paper [19] elaborates the methods for analytical determination of cylindrical sample strength in terms of the truncated-wedge destruction. In this context, we will represent only the end Coulomb formula [15], [19]-[21]:

$$\tau_e \geq k = |\tau_\alpha| - \mu\sigma_\alpha, \qquad (3)$$

where:

τ_e – effective shear stresses (Pa) at a sliding surface (SS);

k – shear strength of a material, Pa;

τ_a – active shear stress, Pa;

μ – internal friction coefficient;

σ_α – normal stress (Pa) on the SS.

Inequality (3) should be understood as follows: the destruction will happen if left side is larger than the right one.

Crack is formed at the SS during the destruction. According to a plain deformation model and while knowing point coordinates of one or two cracks, it is possible to identify bearing share of a sample being equal to the initial area of the latter exclusive of its share which got out of load in the process of a crack development. The sample share which got out of load is defined through abscissa values of the crack point as x-yctg α where y is ordinate of the crack point, m; and α is incidence SS angle (rad) within the crack point towards abscissa axis OX. If σ_y (Pa) stresses within the crack point are known as well as its coordinates and regularities of contact stress distribution within the share which did not get out of the load (i.e. bearing part of the sample), it is possible to identify a strength value of the sample if rates of four property indicators are available. They are shear resistance limit k (Pa); external f_c and internal μ friction coefficients; and elasticity modulus E (Pa). Taking into consideration the symmetry of semicircles of a cylindrical sample cut, calculation is performed for any of them; for instance, the left one (Fig. 1). Subsequently, the specific effort on the bearing share of a cylindrical sample is the true fracture stress at the moment of crack formation:

$$p = \sigma_y \frac{\left(S_0 - \left(\int_0^x F(x)dx + \frac{2f_c}{h} \int_0^x F(x)xdx \right) \right)}{\left(S_0 - \int_0^x F(x)dx \right)_i}, \quad (4)$$

where:

p – specific effort, Pa;

σ_y – standard stress within the crack points, Pa;

S_0 – initial semicircle area, m^2;

$F(x)$ – change function of a semicircle area getting out of load at the moment of crack formation, m^2.

Demonstrate the sample breakage using a scheme in Figure 2. Locate the coordinate axis centre in the top left corner of the sample. Within the upper plain of a left longitudinal sample half, both contact τ_c (Pa) and internal τ_{yx} (Pa) shear stresses are positive; they are negative within the lower plain. On the right half, the signs have opposite values. The truncated-wedge form of rock sample destruction is characterized by lack of SS crossing with a vertical symmetry axis. It crosses lower contact plain.

Since the deformation results in convex shapes of sample edges, apply pairing law of shear stresses within the angular points. Assume that the development of deformations takes place along SS: from the left side along SS ξ_l; and from the right side along SS ξ_r. Taking into consideration SS symmetry, describe formation of the left SS ξ_l. As Formula (4) explains, the computation should involve calculation formulas for stresses within the crack points at the moment of its development. In addition, as it follows from Formula (4), the solution needs knowledge of distribution regularity of the standard contact stresses. Formula (4) implementation involves an expression of parameters of their varying areas through the areal integrals.

It follows from Figure 1 that areal element is equal to a product of a segment chord length by an abscissa differential x:

$$ds = 2\sqrt{ux - x^2}\,dx, \quad (5)$$

where:

u – circle diameter, m.

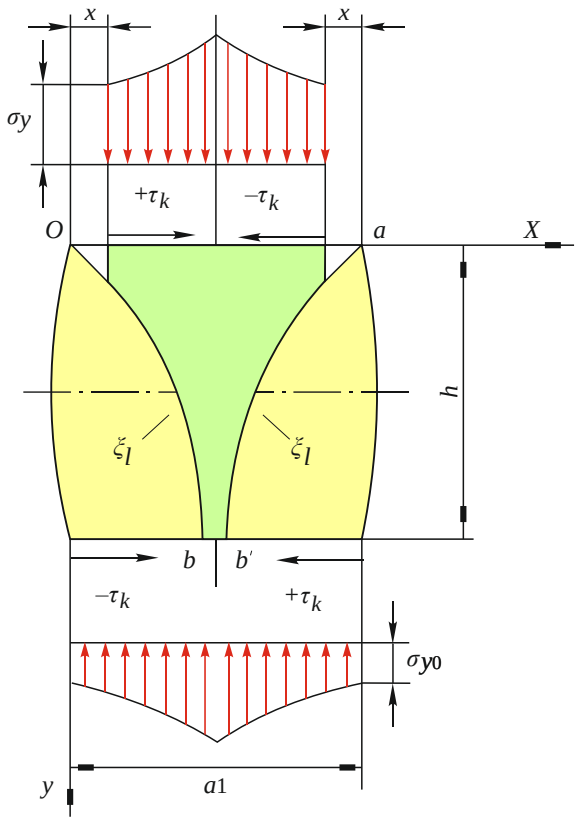

Figure 2. Scheme of standard and contact shear load formation and crack development along the sliding surfaces

Then, represent Formula (2) as follows:

$$\sigma_{yi} = \sigma_{y_0} \left(1 + \frac{4f_c x\sqrt{ux - x^2}}{h} \right). \quad (6)$$

Hence, relying upon Expression (6) and according to Formula (4), define a value of the specific effort on the bearing sample share being equal to $\pi u^2/8$ (i.e. semicircle area) exclusive of an area which got out of the load at the moment of crack formation:

$$p = \sigma_y \frac{\left(\frac{\pi u^2}{8} - \int_0^x \left(1 + \frac{2f_c\, x\sqrt{ux - x^2}}{h} \right) dx \right)}{\left(\frac{\pi u^2}{8} - \int_0^x \sqrt{ux - x^2}\,dx \right)_i}. \quad (7)$$

Using p stress, a line of true stresses is drawn on Formula (7). Relative diagram is recorded on the press since the former registers automatically the stress on the bearing share of the sample; the initial area is assumed while calculating the space. Consequently, the analytical true diagram should be transformed into the relative one while multiplying the specific effort values of the true diagram by bearing area-initial area ratio. It is required to define a value of parameter one being the current value of a sample strength within the evanescent branch. For the purpose, express the area, getting out of the load in the form of a segment (Fig. 1) using the known Formula:

$$S_{ambv} = \frac{\pi u^2}{8}\left(\phi - \sin\phi\right), \quad (8)$$

where:

$$\phi = 2arcsin\sqrt{1-\left(\frac{u-2x_\xi}{u}\right)^2}\ . \quad (9)$$

So, the segment area (Fig. 1) in the process of crack development is:

$$S_i = \frac{\pi u^2}{8}(\phi - \sin\phi) = \frac{\pi u^2}{4}\times$$
$$\times\left(\arcsin 2\sqrt{ux_\xi - x_\xi^2} - 2\left(1-2x_\xi\right)\sqrt{ux_\xi - x_\xi^2}\right). \quad (10)$$

Taking into consideration the fact that semicircle area is $\pi u^2/8$, record the formula to identify strength within the evanescent branch of axial stress-strain diagram in the form of:

$$\sigma_c = \frac{8p}{\pi u^2}\left(\frac{\pi u^2}{8} - \frac{1}{4}\left(\arcsin 2\sqrt{ux_\xi - x_\xi^2} - \right.\right.$$
$$\left.\left. -2\left(1-2x\right)\sqrt{ux_\xi - x_\xi^2}\right)\right). \quad (11)$$

Use a guide [20] to solve Formula (7) integrals.

In such a way, the specific effort on the contact plane will be defined through the Formula:

$$p = \sigma_y\left(\begin{array}{l}\frac{\pi u^2}{8} - \left(-\frac{1}{4}\left(\arcsin 2\sqrt{ux_\xi - x_\xi^2} - 2\left(1-2x_\xi\right)\sqrt{ux_\xi - x_\xi^2}\right)\right) + \\ +2f_c\left(\frac{\left(-ux_\xi + x_\xi^2\right)\sqrt{ux_\xi - x_\xi^2}}{3} + \frac{\left(2x_\xi - u\right)\sqrt{ux_\xi - x_\xi^2}}{8} - \right. \\ \left. \frac{u^2\left(\frac{\pi}{2} - \arcsin 2\sqrt{ux_\xi - x_\xi^2}\right)}{16}\right)\end{array}\right) / \frac{\pi u^2}{8} - \frac{1}{4}\left(\arcsin 2\sqrt{ux_\xi - x_\xi^2} - 2\left(1-2x_\xi\right)\sqrt{ux_\xi - x_\xi^2}\right). \quad (12)$$

Complete problem solution should involve determination of the standard stress σ_y within a crack point for Formula (12). Paper [19] states a method to define the stress relying upon Coulomb criterion; horizontal stresses are ignored. Based upon the balance of forces on the extreme plain, papers [20], [22] derived the expression to calculate the standard horizontal stress, Pa:

$$\sigma_x = \frac{2\left(k+\mu\sigma_y\right)}{\cos\rho}\left(\sin\rho - \sqrt{1-b^2}\right) + \sigma_y\,, \quad (13)$$

where:

$b = f\sigma_y/(k + \mu\sigma_y)$;

ρ = arctg μ are angle and internal friction coefficient, rad.

According to A.D. Tomlyonov and [23], increase in shear resistance within the angular point o (Fig. 2) is defined through the condition that a force application technique cannot influence stress distribution within the sections quite distancing from the application places. The condition is expansion of Saint-Venant's principle used in the elasticity theory. If $x = 0$ in the unloaded section then:

$$\int_0^{h/2}\sigma_x\,dy = 0\,, \quad (14)$$

where:

h – a sample height, m.

While inserting σ_x value (13) into expression (14) after integrating, identify:

$$C = \frac{1}{2}abs\left(k\arcsin\left(\frac{f_c\sigma_y\left(1-\frac{2y}{h}\right)}{k+\mu\sigma_y}\right)\right). \quad (15)$$

To simplify the record in future, introduce the indication:

$$d = \frac{1}{2}\arcsin\left(\frac{f_c\sigma_y\left(1-\frac{2y}{h}\right)}{k+\mu\sigma_y}\right). \quad (16)$$

$f_c\sigma_y\left(1-\frac{2y}{h}\right)$ expression represents shear stress attenuation along y ordinate. According to [18] method, σ_y (Pa) stresses within the crack point on the left SS ξ_l; are identified using the equation system:

$$\sigma_y = \frac{1}{\mu}\left[\frac{\left(k\left(1+\mu d\right)\cdot\left(1+Sin\rho\sqrt{1-b_\xi^2}\right)\right)\cdot\exp\left(2\mu\left(\beta_\xi+\beta_b\right)\right)}{1-Sin\rho\cdot\sqrt{1-b_\xi^2}} - k_b\right], \text{ where:} \quad (17)$$

$$k_b = \frac{\left(k+\mu\sigma_y\right)\left(1-Sin\rho\sqrt{1-b_{\xi'}^2}\right)}{\left(1+\mu d\right)\left(1+Sin\rho\sqrt{1-b_{b_\xi}^2}\right)\cdot\exp\left(4\mu\beta_b\right)}\ ; \quad (18)$$

$$b_\xi = \frac{f_c\left(1-\frac{2y}{h}\right)\cdot\sigma_{y_\xi}\left(1+\frac{2f_c}{h}x_\xi\right)}{k+\mu\cdot\sigma_{y_\xi}\left(1+\frac{2f_c}{h}x_\xi\right)}\ ; \quad (19)$$

$$b_b = -\frac{f_c\cdot\sigma_{y_\xi}\left(1+\frac{2f_c}{h}x_b\right)}{k_b+\mu\cdot\sigma_{y_\xi}\left(1+\frac{2f_c}{h}x_b\right)}\ ; \quad (20)$$

$$\beta_\xi = \frac{1}{2}\text{arctg}\frac{b_\xi\cos\rho}{\sin\rho-\sqrt{1-b_\xi^2}}\ ; \quad (21)$$

$$\beta_b = \frac{1}{2}\text{arctg}\frac{b_b \cos\rho}{\sin\rho - \sqrt{1-b_b^2}}, \quad (22)$$

where:

k_b – effective shear stress within b point of SS ξ emergence to the contact surface, Pa (Fig. 2);

x_b – b point abscissa, m;

β_ξ and β_b – rotation angles of SS ξ within the crack point, and within b point respectively, rad.

SS ξ incidence angle α (rad) is defined through the Formula:

$$\alpha_\xi = \frac{\pi}{4} + \frac{\rho}{2} + \beta_\xi, \quad (23)$$

where:

ρ = arctg μ is internal friction angle, rad.

Apply Hooke law to identify deformations being parameter two of the diagram. Taking into consideration the standard horizontal stresses, the formula to calculate deformations is as:

$$\varepsilon = \frac{p - \nu\sigma_x}{E}, \quad (24)$$

where:

v – Poisson ratio;

E – elasticity modulus, Pa.

Use of Formula (11) in addition to (12-24) Expressions makes it possible to apply iteration method to identify on the PC parameters of the true and conditional axial stress-deformation diagrams obtained by researchers with the help of presses under the truncated-wedge destruction of cylindrical samples in the form of an evanescent branch function.

Determine the basic regularities of a sample destruction process based upon the abovementioned. Take following conditions as an example: k = 22 MPa; 40° (μ = 0.839); and f_c = 0.25. In the context of boundary conditions, contact friction f_c is among the most important parameters. According to Saint Venant principle, friction attenuates in terms of certain rule while distancing from a contact surface [23]. Along the normal stress action through a body, researchers have adopted a linear law of contact shear stress attenuation under the formula $f_i\sigma_y = f_c\sigma_y\left(1-\frac{2y}{h}\right)$. Prandtl has proved that in our situation, the normal σ_y stress cannot depend upon an ordinate. Consequently, dependence of the contact shear stresses upon the contact friction coefficient becomes obvious.

To calculate destruction parameters within the progressive crack point, programs have been developed for PC involving (14)-(22) Equation system to solve the problems using iteration method. Vertically, computer screen was divided into 8 lines; horizontally, it was divided into 12 columns.

3. Results and their discussion

The calculation has helped identify that a contact friction coefficient within a crack point depends linearly upon the ordinate of a sample crack point (Fig. 3, straight *1*) while changing a positive sign to the negative one within the horizontal axis of symmetry. The regularity is also typical for rotation SS β_ξ angle with negative sign change to a positive one (Fig. 3, straight *2*). The angle depends directly upon a friction coefficient variation. β_b angle (Fig. 3, straight *3*) is a constant value since it represents rate of SS rotation angle within one point of its emergence within the lower contact surface. Inclination SS α angle (Fig. 3, straight *4*) of an ordinate is of increasing nature.

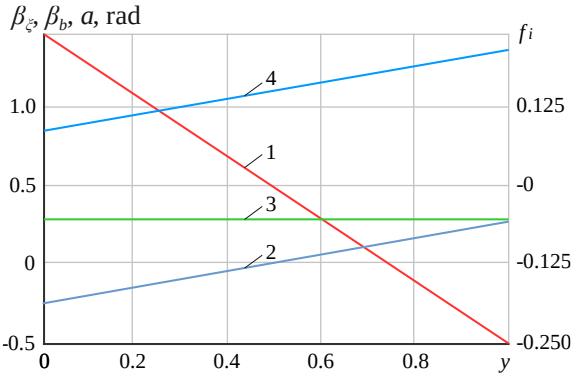

Figure 3. Dependencies of a contact friction coefficient, rotation angles, and inclination SS ξ angles of the crack point ordinate if k_n = 10 MPa, ρ = 40° and f_c = 0.25: 1 – contact friction coefficient f_i; 2 – rotation angle β_ξ; 3 – rotation angle β_b; 4 – inclination angle α

Values of the geometrical parameters form the numerical abscissa values of a crack point x as well as power parameters depending upon the values of a crack point ordinate (Fig. 4). The geometrical parameters also involve the bearing area dependence, i.e. a sample area which got beyond load during the crack progress. Relying upon Formula (11), where p parameter is excluded, we define the bearing area dependence on the ordinate (Fig. 4).

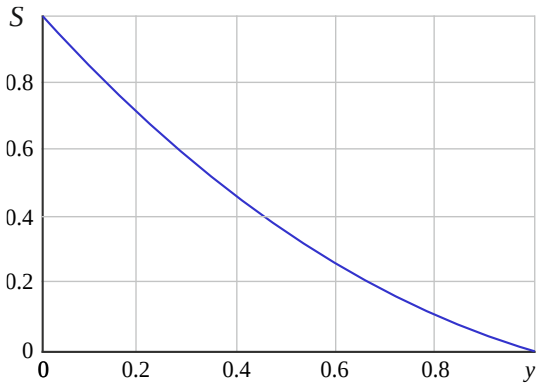

Figure 4. Dependence of a relative sample bearing area upon a crack point ordinate if k = 10 MPa; ρ = 40° and f_c = 0.25

Identify regularities of power parameters of the crack point ordinate value (Fig. 5). Abscissa of the crack point is defined through $x = ytg\alpha$ formula (curve *1*). Equation system (14-22) helps identify vertical stresses σ_y since the formulas have linear regularity to be increased (straight *2*). k_b parameter of effective shear stresses within the point of SS getting to the lower contact surface is defined using Formula (18). Dependence of k_b parameter is expressed through the increasing quadratic function (curve *3*). Its values within the end point are equal to shear strength of the destructed material k. Contact shear stresses inside the sample form standard horizontal stresses σ_x defined using Formula (13). Now, describe the last-mentioned important parameter (i.e. specific effort p) identified through Formula (12). The specific effort determines the stress acting at the surface of the bearing share of the sample.

Use of Formula (11) in addition to (12)-(24) Expressions makes it possible to apply iteration method to identify on the PC parameters of the true and conditional axial stress-deformation diagrams obtained by researchers with the help of presses under the truncated-wedge destruction of cylindrical samples in the form of an evanescent branch function $\sigma_c = \psi(\varepsilon)$ (Fig. 6).

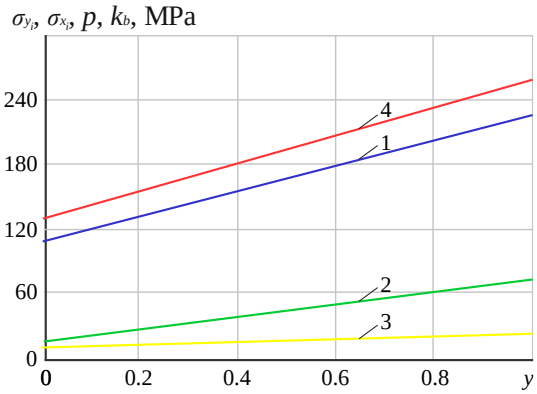

Figure 5. Dependencies of vertical standard stresses σ_y; reference shear stresses k_b; standard horizontal stresses σ_x; and specific efforts p within the crack point upon the crack ordinate if k_n = 10 MPa; ρ = 40° and f_c = 0.25: 1 – vertical standard stresses σ_y; 2 – horizontal standard stresses σ_x; 3 – reference shear stresses k_b; 4 – specific efforts p

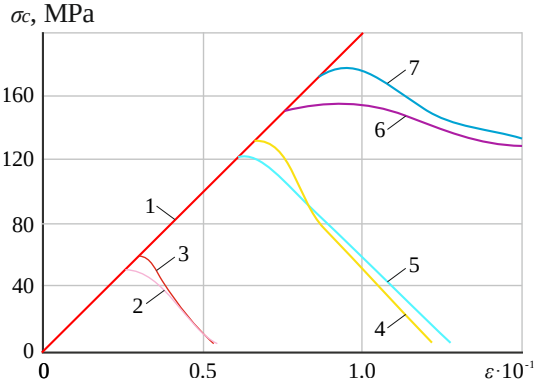

Figure 6. Stress-strain diagrams of cylindrical samples under the truncated-wedge destruction of cylindrical samples if f_c = 0.25 and E = 2000 MPa: 1 – true diagram; (2)-(7) – conditional diagrams: (2) if k = 10 MPa and ρ = 40°; (3) if k = 10 MPa and ρ = 40° taking into consideration σ_x; (4) if k = 22 MPa and ρ = 40°; (5) if k = 22 MPa and ρ = 40° taking into consideration σ_x; (6) if k = 22 MPa and ρ = 50°; (7) if k = 22 MPa and ρ = 50° taking into consideration σ_x

Figure 6 demonstrates the functions in terms of different values of rock characteristics for the samples which height diameters are equal to unity. Analysis of the diagrams helps draw the important conclusion: inclination angle of evanescent curve $\sigma_c = \psi(\varepsilon)$, being so-called decreasing modulus M assumed by researchers as a constant material characteristic similarly to elasticity modulus E [3], [13], depends upon numerical values of rock characteristics; it is not a constant. Many authors [3], [13] explain roundness of evanescent branches right beyond the elastic strength by rock plasticity. In our opinion, the roundness results from contact friction and crack geometry.

The calculations support the idea that the truncated-wedge destruction takes place if $\rho > 39°$ and f_c is within 0.2-0.4. In the context of the truncated-wedge destruction, compare the values of analytical strength of cylindrical samples which height and diameter are equal to unity, with the experimental data borrowed from rock cadastre [24] obtained by researchers with the help of presses. The cadastre contains uniaxial compression data, rock shear strength data, and internal friction angle. The comparison between analytical strength and experimental data is summarized in Table 1 (rock ranking depending upon shear strength).

Comparison between analytical data and experimental ones has shown that average variation coefficient is 12.5% if the standard horizontal stresses are ignored; the figure is 9.7% if they are taken into consideration. Correlation between analytical strength and experimental data confirms high efficiency of the proposed technique to calculate strength of rock cylindrical samples. The abovementioned permits us to recommend the procedure for mining enterprises if it is required to identify rock strength.

Consequently, the proposed analytical diagramming technique based upon four physicomechanical rock characteristics, easily identifiable by experiments, will help mining enterprises determine more accurately stress-strain state of rock mass and evaluate stability of underground structures especially within the face areas. The characteristics are also applicable for mineral processing specifically to prepare ore materials for mining and smelting procedures; prepare building materials; for chemical production to improve the efficiency of rock mass and another hard material destruction with energy saving to disintegrate minerals in mines; open pits; at mining and processing integration works; and at stone-processing enterprises. They also can be used while processing structural components under emergency and other force majeure situations.

Further studies of frictional characteristics of rocks (especially if their impact by working organs of machines is taken into consideration under asymmetric or more complex force application) may result in significant reduction of energy consumption for disintegration in the processes of mineral preparation.

4. Conclusions

Analytical procedure to identify the parameters of axial stress-deformation diagrams under the truncated-wedge destruction of cylindrical rock samples has been improved with the use of their four experimental characteristics (k being shear resistance; f_c and μ being coefficients of contact and internal friction; and E being elasticity modulus) which can be identified in the laboratories of mining enterprises. The technique advantage is prompt use of the calculation results in a production environment.

The method is based upon a new, physically more substantiated formula of the standard contact stress distribution to compare with the available ones; moreover, it takes into consideration values of the standard horizontal stresses resulting from contact friction between a press plate and a sample. The technique helps improve reliability of parameter computation in the context of standard stress-axial deformation diagrams for the truncated-wedge destruction of cylindrical rock samples.

The developed method identifying parameters of standard stress-axial deformation diagrams for the truncated-wedge destruction of cylindrical rock samples is recommended to be applied by mining enterprises while rock strength determining. The truncated-wedge destruction shape of samples is formed if $\rho > 39°$ and f_c is within 0.2-0.4.

Acknowledgements

The authors express their gratitude to V.V. Vynohradov, Doctor of Engineering, Professor, Deputy Director of the Institute of Geotechnical Mechanics named by N. Poljakov for the statement of the research problem.

Table 1. Comparison of analytical strength of cylindrical samples and experimental data

Rock	Shear strength k, MPa	Internal friction angle ρ, rad	Experimental strength limit σ_e, MPa	Analytical strength limit		Variation coefficient		Guide of physical characteristics of rocks [24]
				ignoring horizontal stresses σ_1, MPa	taking into consideration horizontal stresses σ_2, MPa	% in terms of σ_1	% in terms of σ_2	
Monazite	5.0	47	35.0	32.8	36.2	6.3	3.4	104
Monzonite	5.2	51	33.0	37.6	41.6	13.9	26.1	105
Aleurite	5.3	45	37.5	33.1	36.5	117	2.7	145
Aleurite	5.33	45	37.5	33.4	36.6	10.9	2.4	209
Monzonite	5.5	49	34.0	37.9	41.8	11,5	22.9	104
Monzonite	7.5	52	61.0	56.1	62.0	8.0	1.6	103
Heavily modified Monazite	7.5	52	66.0	56.1	62.0	15.0	6.1	104
Monzonite	8.5	41	47.0	48.5	53.4	3.2	13.6	103
Sandstone	8.8	43	61.5	52.6	59.6	14.5	3.1	161
Aleurite	9.6	43	62.0	57.4	63.3	7.4	2.1	145
Sandstone	9.72	50	81.5	68.8	75.8	15.6	7.0	145
Black iron ore	10.0	45	86.1	62.0	68.9	30.0	19.9	67
Monzonite	10.5	52	85.0	78.6	86.5	7.5	1.8	104
Garnet-magnetite scarn	12.0	42	97.0	70.0	77.0	27.8	20.6	67
Aleurite	12.0	42	75.5	70.0	77.0	7.3	2.0	208
Quartz	12.5	44	100.0	76.6	84.6	23.4	16.0	103
Black iron ore	15.0	42	97.0	87.6	94.4	9.7	2,7	67
Sandstone	16.5	42	126.0	96.4	106.4	23.5	15.6	145
Sandstone	17.4	49	126.0	120.0	132.3	4.8	5.0	161
Garnet-magnetite ore	22.0	40	117.0	122.0	135.4	4.3	15.7	67
Monzonite	24.0	40	134.2	134.0	147.0	0.1	9.5	105
Monzonite	28.0	52	164.0	209.4	207.4	27.7	26.5	104
Sandstone	28.5	45	200.0	178.4	196.0	10.8	2.0	161
Monzonite	60.0	41	365.0	343.0	377.0	6.0	3.3	104

References

[1] Zhang, L., Cao, P., & Radha, K.C. (2010). Evaluation of rock strength criteria for wellbore stability analysis. *International Journal of Rock Mechanics and Mining Sciences*, *47*(8), 1304-1316. https://doi.org/10.1016/j.ijrmms.2010.09.001

[2] Sdvyzhkova, O., Bфиуеіб Вю, Moldabayev, S., Rysbekov, K., & Sarybayev, M. (2020). Mathematical modeling a stochastic variation of rock properties at an excavation design. *Proceedings of the 20th International Multidisciplinary Scientific GeoConference: Science and Technologies in Geology, Exploration and Mining*, 165-172. https://doi.org/10.5593/sgem2020/1.2/s03.021

[3] Blokhin, V.S., Bolshakov, V.I., & Malich, N.G. (2006). *Osnovnye parametry tekhnologicheskikh mashin. Mashiny dlya dezintegratsii tverdykh materialov*. Dnepropetrovsk, Ukraina: IMA-press, 404 s.

[4] Nesmashnyy, E.A. (2001). *Optimizatsiya geometricheskiikh parametrov otkrytykh gornykh vyrabotok*. Krivoy Rog, Ukraina: Mineral, 118 s.

[5] Nesmashnyy, E.A., & Bolotnikov, A.V. (2017). Opredeleniye prochnosti skalnykh porod s ispolzovaniyem sovremennogo oborudovaniya na primere mestorozhdeniya "Bolshaya Glivatka". *Metallurgicheskaya i Gornorudnaya Promyshlennost'*, (3), 82-87.

[6] Huang, B., & Liu, J. (2013). The effect of loading rate on the behavior of samples composed of coal and rock. *International Journal of Rock Mechanics and Mining Sciences*, (61), 23-30. https://doi.org/10.1016/j.ijrmms.2013.02.002

[7] Vinogradov, V.V. (1989). *Geomekhanika upravleniya sostoyaniyem massiva vblizi gornykh vyrabotok*. Kiev, Ukraina: Naukova dumka, 192 s.

[8] You, M. (2010). Mechanical characteristics of the exponential strength criterion under conventional triaxial stresses. *International Journal of Rock Mechanics and Mining Sciences*, *47*(2), 195-204. https://doi.org/10.1016/j.ijrmms.2009.12.006

[9] Meyer, J.P., & Labuz, J.F. (2013). Linear failure criteria with three principal stresses. *International Journal of Rock Mechanics and Mining Sciences*, (60), 180187. https://doi.org/10.1016/j.ijrmms.2012.12.040

[10] Bartashchuk, O. (2016). Systemna orhanizatsiia dyziunktyvnoi tektoniky konsolidovanoho fundamentu Dniprovsko-Donetskoho paleoryftu. Chastyna 1. Lineamenty. *Visnyk KhNU, Seriia "Heolohiia, Heohrafiia, Ekolohiia"*, (45), 14-22.

[11] Kalchuk, S.V. (2011). Vplyv tektonichnykh syl na formuvannia napruzheno-deformovanoho stanu porid rodovyshch blochnoho oblytsiuvalnoho kameniu. *Visnyk ZhDTU*, (1), 162-165.

[12] Shmatovskiy, L.D., Girich, E.G., & Pozhitko, I.I. (2002). Opyt podgotovki i ispolzovaniya gidravlicheskogo oborudovaniya dlya otsenki napryazhennogo sostoyaniya ugleporodnogo massiva plasta. *Heotekhnichna Mekhanika*, (37), 104-109.

[13] Henning, J.G., & Mitri, H.S. (2007). Numerical modelling of ore dilution in blasthole stoping. *International Journal of Rock Mechanics and Mining Sciences*, *44*(5), 692-703. https://doi.org/10.1016/j.ijrmms.2006.11.002

[14] Sdvyzhkova, O., Golovko, Y., & Klymenko, D. (2017). Effect of harmonic oscillations on a crack initiation in the rock mass. *Naukovyi Visnyk Natsionalnoho Hirnychoho Universytetu*, (4), 13-18.

[15] Chanyshev, A.I. (2010). Zapredelnoe deformirovanie materialov pri antiploskoy deformatsii i ego uchet v zadache o rasprostranenii pryamolineynoy polubeskonechnoy treshchiny. *Deformirovanie i Razrushenie Materialov s Defektami i Dinamicheskie Yavleniya v Gornykh Porodakh i Vyrabotkakh*, 349-354.

[16] Davydenko, O.M., & Ihnatov, A.O. (2019). Mekhanika efektyvnoho ruinuvannia hirskykh porid sharoshkovo-lantsiuhovymy dolotamy. *Porodorazrushayushchiy i Metalloobrabatyvayushchiy Instrument – Tekhnika i Tekhnologiya ego Izgotovleniya i Primeneniya*, (22), 148-157.

[17] Olovyannyy, A.G. (2012). *Mekhanika gornykh porod. Modelirovaniye razrusheniy*. Sankt-Peterburg, Rossiya: Kosta, 280 s.

[18] Vasilyev, L.M., Vasilyev, D.L., Malich, N.G., & Angelovskiy, A.A. (2018). *Mekhanika obrazovaniya form razrusheniya obraztsov gornykh porod pri ikh szhatii*. Dnepr, Ukraina: IMA-press, 174 s.

[19] Vasyliev, L.M., Vasyliev, D.L., Nazarov, O.Ye., Malich, M.G., & Katan, V.O. (2021). The method for determining the parameters of the diagrams of a truncated-wedge destruction of cylindrical samples of rocks. *Naukovyi Visnyk Natsionalnoho Hirnychoho Universytetu*, (1), 47-52. https://doi.org/10.33271/nvngu/2021-1/047

[20] Bronshteyn, I.N., & Semendyayev. L.A. (1964). *Spravochnik po matematike*. Moskva, Rossiya: Nauka, 608 s.

[21] Vasilyev, L.M., & Vasilyev, D.L. (2013). Teoreticheskoe obosnovanie formirovaniya gorizontalnykh normalnykh napryazheniy v massivakh

gornykh porod. *Fiziko-Tekhnicheskie Problemy Razrabotki Poleznykh Iskopayemykh*, (2), 81-90.

[22] Vasil'ev, L.M., & Vasil'ev, D.L. (2013). Theoretical ground for origination of normal horizontal stresses in rock masses. *Journal of Mining Science*, *49*(2), 240-247. https://doi.org/10.1134/s1062739149020056

[23] Chykhladze, E.D., Verevicheva, M.A., & Halahuria, Ye.I. (2010). *Osnovy liniinoi teorii pruzhnosti, plastychnosti ta povzuchosti*. Kharkiv, Ukraina: UkrDAZT, 149 s.

[24] Melnikov, N.V., & Rzhevskiy, V.V. (1975). *Spravochnik (kadastr) fizicheskikh svoystv gornykh porod*. Moskva, Rossiya: Nedra, 279 s.

Вдосконалення методу розрахунку міцності циліндричних зразків гірничих порід при одноосному стисканні

Л. Васильєв, М. Маліч, Д. Васильєв, В. Катан, З. Різо

Мета. Удосконалення аналітичного методу розрахунку межі міцності циліндричних зразків гірських порід при врахуванні горизонтальних нормальних напружень.

Методика. Математичне моделювання процесу руйнування циліндричних зразків гірських порід на прикладі усічено-клинової форми руйнування здійснювалося з урахуванням горизонтальних нормальних напружень із використанням чотирьох експериментальних характеристик (k – межі міцності зсуву, f_c і μ – коефіцієнтів контактного та внутрішнього тертя, E – модуля пружності) та зіставлення розрахункових меж міцності з експериментальними даними, отриманими при одновісному стисканні.

Результати. Метод дозволяє визначити межу міцності та залишкову міцність циліндричних зразків гірських порід із використанням чотирьох показників властивостей, які простими способами можуть бути встановлені експериментально. Зіставлення розрахункових меж міцності з експериментальними даними, отриманими при одновісному стисканні, свідчить про високу результативність запропонованого методу.

Наукова новизна. Перевагою методу є можливість оперативного використання результатів розрахунку на виробничих підприємствах, тому що в їх умовах простими способами можуть бути визначені показники фізико-механічних властивостей гірських порід для визначення стійкості підземних споруд у шахтах та зниження енерговитрат при дезінтеграції на кар'єрах та ГЗК.

Практична значимість. Вперше проведено аналітичне моделювання процесу руйнування циліндричних зразків гірських порід на прикладі усічено-клинової форми руйнування з урахуванням горизонтальних нормальних напружень, а також внутрішнього і зовнішнього тертя.

Ключові слова: *гірська порода, межа міцності, руйнування, тріщина, напруження, одноосне стискання*